Fish and Shellfish Immunology 91 (2019) 19–28

Contents lists available at ScienceDirect

Fish and Shellfish Immunology

journal homepage: www.elsevier.com/locate/fsi

Full length article

# Molecular characterization and expression analysis of dopa decarboxylase involved in the antibacterial innate immunity of the freshwater crayfish, *Procambarus clarkii*

Kai Wang[a,1], Qian Ren[b,c,1], Xiu-li Shen[d,1], Bo Li[a], Jie Du[a], Xiao-dong Yu[a], Zhi-qiang Du[a,*]

[a] *School of Life Science and Technology, Inner Mongolia University of Science and Technology, Baotou, Inner Mongolia Autonomous Region, 014010, China*
[b] *Co-Innovation Center for Marine Bio-Industry Technology of Jiangsu Province, Lianyungang, 222005, China*
[c] *College of Marine Science and Engineering, Nanjing Normal University, Nanjing, 210046, China*
[d] *Library, Inner Mongolia University of Science and Technology, Baotou, Inner Mongolia Autonomous Region, 014010, China*

ARTICLE INFO

*Keywords:*
*Procambarus clarkii*
*Dopa decarboxylase*
RNAi
Antibacterial innate immune
Neuroendocrine-immune (NEI) system

ABSTRACT

Dopa decarboxylase (DDC) is responsible for the synthesis of dopamine, which acts as an important modulator in the nervous systems of vertebrates and invertebrates. Recent studies have indicated that DDC also plays crucial roles in the insect innate immune system. However, the functions of DDC in immunomodulation in crustaceans have not been thoroughly elucidated to date. In this study, a new full-length cDNA of the DDC protein was identified from red swamp crayfish, *Procambarus clarkii* (named *Pc-ddc*). The ORF of *Pc-ddc* encoded 474 amino acids, which possessed a 377-amino-acid domain. *Pc-ddc* was expressed at a relatively high level in the hemocytes and gills of crayfish. This protein was expressed at a relatively low level in the hepatopancreas and intestine. The expression level of *Pc-ddc* was clearly upregulated in hemocytes, hepatopancreas, gills, and intestine tissues after challenge with *S. aureus* or *E. ictaluri*. The results of the enzyme catalysis assay showed that the enzyme catalysis activity of r*Pc*-DDC was 35 ± 2.8 ng $h^{-1}$ $mg^{-1}$ (n = 3). In addition, the results of the mimetic crayfish hemocytes encapsulation assay showed that the encapsulation rate of beads coated with r*Pc*-DDC was clearly increased. The results of the bacterial binding assay showed that r*Pc*-DDC strongly binds to *S. aureus* and *E. ictaluri*. Finally, when *Pc-ddc* was knocked down, the number of surviving crayfish clearly decreased after *S. aureus* or *E. ictaluri* was injected. All of these results indicate that *Pc*-DDC is an important immunomodulating enzyme in the neuroendocrine-immune (NEI) system of crayfish.

## 1. Introduction

In invertebrates, phagocytosis, nodulation, encapsulation, and melanization are crucial innate immune responses that are used to defend against pathogens [1]. At present, it is clear that the occurrence of melanization is mediated by the prophenoloxidase (proPO) activation system [2]. This system is triggered by several bacterial cell wall components, such as glucan, LPS and peptidoglycans [3,4]. Activated phenoloxidase (PO), which is the last component of the proPO activation system, catalyzes the hydroxylation reaction of tyrosine to transform dihydroxy-phenyl-alanine (dopa) [5]. Subsequently, dopa is decarboxylated by dopa decarboxylase (DDC) to transform dopamine, which is a vital signal molecule in the neuroendocrine system [6]. Dopamine not only plays the crucial roles of the neurotransmitter and hormone in the neuroendocrine systems of vertebrates but also plays important roles in the innate immune systems of invertebrates [7]. In humans, dopamine plays a critical role in cognition, learning and behavior by regulating some associated neural activities [8]. Metabolic disorders of dopamine seriously affect mammalian brain functions. For example, both Alzheimer's disease and Parkinson's disease are related to dopamine metabolic abnormalities [9]. In insects, dopamine is crucial for both sclerotization and melanization, which are important for exoskeleton formation and innate immune function [10].

By catalyzing dopamine production, DDC is also functionally related to neurological disorders and plays an important role in brain development in humans. DDC is responsible for the decarboxylation step in catecholamine and dopamine biosynthesis [11]. The activity of DDC is adjusted in the rodent brain by enzyme activation and induction [12]. In invertebrates, accumulating evidence demonstrates that DDC plays a crucial role in the intricate neuroendocrine immune (NEI) system [13].

---

[*] Corresponding author.
*E-mail address:* nmdzq1981@163.com (Z.-q. Du).
[1] These authors contributed equally to this work.

https://doi.org/10.1016/j.fsi.2019.05.013
Received 28 January 2019; Received in revised form 27 April 2019; Accepted 7 May 2019

This protein catalyzes the production of the neurotransmitters dopamine and serotonin and is involved in melanization, wound healing, cuticle hardening, and parasite defense of insects [14]. DDC is a multifunctional enzyme in the innate immune system. For example, *Bm*-DDC is the key enzyme in the *Bombyx mori* molting process, and it is directly related to the regulation of ecdysone [15]. In *Tribolium castaneum*, *Tc*-DDC is involved in the cuticle tanning process [16]. An RNAi assay performed on *Tc*-DDC demonstrated that a lethal pupal phenotype was produced after ds*Tc*-DDC was injected into larvae. Because this protein participates in the synthesis of dopamine, which is metabolized to produce reactive quinines, *Dm*-DDC is involved in the killing effects on invading bacteria in the epidermis of *Drosophila melanogaster* [17]. In *Anopheles gambiae*, knockdown of *Ag*-DDC via the RNAi assay leads to a significant decrease in melanization. *Ag*-DDC is believed to be involved in accelerating the formation of melanin [18]. In *Chlamys farreri*, *Cf*-DDC modulates innate immune responses through its catalytic activity, including hemocytes encapsulation and regulation of the ROS level [6]. Additionally, this protein acts as an essential immunomodulating enzyme in the NEI system of scallop.

Red swamp crayfish (*Procambarus clarkii*) has been broadly cultivated in China. Due to this crayfish's superior disease resistance, it has become a vital economic aquaculture animal [19]. Crayfish have been frequently used as a model organism to research the molecular mechanisms of the innate immune system [20]. The abovementioned research results on DDC mainly focused on the identification, characterization, and mRNA expression levels in certain insects, such as *B. mori*, *T. castaneum*, *D. melanogaster*, and *A. gambiae*. In contrast to insects, relatively little is known about DDC in crustaceans. In the present study, a novel full-length cDNA of DDC protein was identified from red swamp crayfish, *Procambarus clarkii* (named *Pc-ddc*). The expression profiles of *Pc-ddc* were detected in hemocytes, hepatopancreas, gills, and intestine in response to bacterial infection. In addition, the enzyme catalysis activity, hemocytes encapsulation function, and bacterial binding activity of r*Pc*-DDC were tested. Finally, the results of the RNAi assay showed that the rate of surviving crayfish was clearly decreased after *S. aureus* or *E. ictaluri* was injected when *Pc-ddc* was knocked down. Taken together, these results revealed that *Pc-ddc* was involved in the antibacterial innate immunity of crayfish.

## 2. Materials and methods

### 2.1. Immunity challenge and tissue collection

*P. clarkii* (weighing approximately 15–20 g each) were bought from an aquatic market in Baotou city, Inner Mongolia Autonomous Region, China. These crayfish were cultivated temporarily in laboratory tanks filled with fresh water for two weeks. The crayfish were fed twice a day with artificial food during the entire experiment [19]. Then, 120 crayfish were chosen and divided into two groups on average. For the bacteria-challenged experiment, *Staphylococcus aureus* or *Edwardsiella ictaluri* ($2 \times 10^7$ cells per crayfish) was injected into the abdominal segment of each crayfish in each group [21]. Subsequently, hemolymph was extracted from the ventral sinus at different time points (2, 6, 12, 24, 36, and 48 h) after bacterial injection using a 5-ml sterile syringe preloaded with 800 μl anticoagulant (10% sodium citrate, pH 7). Hemolymph was centrifuged immediately at 800 × *g* for 5 min (4 °C) to isolate hemocytes [22]. Other tissues from bacteria-challenged crayfish, such as hepatopancreas, gills, and intestine, were also collected at different time points (2, 6, 12, 24, 36, and 48 h) after bacterial infection for the purpose of RNA extraction. In addition, hemolymph and other normal tissues (hepatopancreas, gills, and intestine) from unchallenged crayfish were also collected using the same method. For unchallenged crayfish, normal crayfish were left untreated. Three parallel experiments were performed to improve the integrity of the work.

### 2.2. RNA extraction and cDNA synthesis

Total RNA of four tissues (hemocytes, hepatopancreas, gills, and intestine) from unchallenged crayfish and bacteria-challenged crayfish at different time points were extracted using RNAiso Plus DNase I (Promega, USA) according to the manufacturer's protocol. Then, the samples were dissolved in DEPC-treated water. Electrophoresis on 1% agarose gel free of RNase was carried out to test the quality of the RNA. At the same time, the quality of RNA samples was also determined with a Nanodrop spectrophotometer (Nanodrop Technologies, USA).

First-strand cDNA synthesis was performed with the Thermo Scientific RevertAid First Stand cDNA Synthesis Kit. According to the protocol, the reaction was finished in 25 μl reaction volume containing 5 μg RNA, 1 μl M-MLV reverse transcriptase (Promega, USA), 1 mM dNTP mixture using SMART F (5′-tac ggc tgc gag aag acg aca gaa ggg-3′), and oligo anchor R (5′-gac cac gcg tat cga tgt cga ct$_{16}$v-3′) at 42 °C for 2 h [23]. Finally, PCR amplification for the *Pc-ddc* partial sequence was carried out to test cDNA quality. The cDNA samples were temporarily stored in a −80 °C cryogenic refrigerator.

### 2.3. Gene cloning

The specific forward and reverse primers (F1:5′-gtc atc ctg acc cag ctg ct-3′; R1:5′-ggt atg gta gtt gag tg-3′) were designed based on the nucleotide sequences of an Expressed Sequence Tag (EST) obtained from our previous transcriptome sequencing [24]. The F1 and 3′ anchor R primers (5′-gac cac gcg tat cga tgt cga c-3′) were used to amplify the 3′ end of the cDNA. The 5′ PCR primer (5′-tac ggc tgc gag aag acg aca gaa-3′) and R1 were used to amplify the 5′ end of the cDNA. Polymerase chain reaction (PCR) amplification was carried out as follows: a cycle of 95 °C for 3 min and 35 cycles of 95 °C for 30 s, 58 °C for 45 s, and 72 °C for 120 s, followed by an additional extension at 72 °C for 10 min. PCR products were gel-purified using the gel purification kit (Sangon, China) as described in the manufacturer's protocol, followed by ligation into the pMD-18T vector (Takara, Japan) and transformation into competent DH5α cells [25]. The positive recombinants were identified through blue-white color selection on ampicillin-containing LB plates and PCR screening using the two specific primers (F1 and R1). Positive clones were sequenced by Sangon (Shanghai, China).

### 2.4. Sequence blast and phylogenic analysis

The similarity between the target protein molecule and other DDC molecules was analyzed using the Web-based Basic Local Alignment Search Tool (BLAST) (http://blast.ncbi.nlm.nih.gov/Blast.cgi). Translation of the amino acid sequences and prediction of the deduced protein were performed on ExPASy (http://www.expasy.org). Alignment with the homogenous sequences from other species was performed using MEGA 7.0. Phylogenic analysis was similarly carried out using Neighbor Joining (NJ) methods of MEGA 7.0 based on the amino acid sequences. To assess the reliability, 1000 bootstraps were selected for the NJ tree [26].

### 2.5. Quantitative real-time PCR analysis for expression profiles of the *Pc-ddc* gene

Total RNA was extracted from different tissues of normal crayfish and bacteria-challenged crayfish at 2, 6, 12, 24, 36, and 48 h time points. Then, RNA (5 μg) from each tissue was used to reverse-transcribe the first strand of cDNA, which was used as a template in PCRs. For quantitative real-time PCR (qRT-PCR) analysis, cDNA templates were diluted 40-fold in nuclease-free water and were used as templates. A pair of primers (*Pc-ddc*-RT-F: 5′-cag cta gat att tga tag c-3′; *Pc-ddc*-RT-R: 5′-ctg tga tga taa cta agt ac-3′) were used in qRT-PCR. The specific primers, *18S RNA*-RT-F (5′-tct tct tag agg gat tag cgg-3′) and *18S RNA*-RT-R (5′-aag ggg att gaa cgg gtt a-3′), were used to amplify the *18S RNA* gene as the inner control.

qRT-PCR was performed following the manufacturer's instructions of SYBR Premix Ex Taq (Takara, Japan) using a real-time thermal cycler (Bio-Rad, USA) in a total volume of 10 μl containing 5 μl of 2 × Premix Ex Taq, 1 μl of the 1:40 diluted cDNA, and 2 μl (1 μM) of each of the forward and reverse primers [19]. The amplification procedure consisted of an initial denaturation step at 95 °C for 3 min and then 40 cycles of 95 °C for 15 s and 57 °C for 30 s, followed by melting from 65 °C to 95 °C. To confirm that only one fragment was amplified, the melting curve was also analyzed for amplification products and was performed at the end of each PCR [23]. Three parallel experiments were performed to increase the integrity (the immunity challenge, total RNA extraction, cDNA synthesis, and qRT-PCR were repeated three times).

Subsequently, inner gene validation was carried out in the current experiment under identical conditions. The *β-actin* and *GAPDH* genes of crayfish were also used as internal controls to study the expression profiles of target genes. The immunity challenge, tissue collection, RNA extraction, cDNA synthesis, and qRT-PCR were performed again. Furthermore, the expression level of the *Pc-ddc* gene was shown as relative expression values, which were calculated according to $2^{-\Delta\Delta CT}$ [19]. The data were subjected to statistical analysis followed by an unpaired sample *t*-test. A significant difference was accepted at $P < 0.05$. Extremely significant difference was accepted at $P < 0.01$.

### 2.6. Recombinant expression and purification

The recombinant expression method can be briefly described as follows. The mature *Pc*-DDC was amplified by the specific expression primers (*Pc-ddc*-exp-F: 5′-tac tca gaa ttc atg gac gcc gat cag ttc-3′, *Pc-ddc*-exp-R: 5′-tac tca ctc gag ctc ctg cag aat gat ctc-3′; *Eco*R I and *Xho* I sites were underlined). pET-28-a (+)-*Pc-ddc* was constructed and generated by subcloning corresponding mature cDNA into the *Eco*R I and *Xho* I sites of pET-28-a. Then, the pET-28-a expression vector carrying the target gene was transformed into competent *E. coli* BL21 (DE3) expression bacteria with kanamycin resistance for recombinant expression [27].

Subsequently, His-Bind resin chromatography (Novagen, Billerica, MA, USA) was used to perform protein purification. Briefly, 2 mL transformant cultured overnight was transferred into 200 mL Luria-Bertani broth containing kanamycin for large-scale culture. When the $OD_{600}$ value reached approximately 0.6, 0.5 mM isopropyl β-D-1-thiogalactopyranoside (IPTG) was added to induce the expression of the target recombinant protein. After culturing at 37 °C for 4 h, the bacteria were collected by centrifugation at 4000*g* for 5 min and resuspended in 20 mL 1 × phosphate-buffered saline (PBS) containing 0.2% Triton X-100. The bacterial pellet was lysed by ultrasonication. The soluble fraction was used for protein purification with His-Bind resin chromatography based on the manufacturer's instructions [19]. Finally, purified recombinant protein was stored at −80 °C until use.

### 2.7. Antibody preparation and western blot analysis

Purified recombinant protein was used as a protein antigen to produce polyclonal *Oryctolagus cuniculus* antiserum using a previously described method [28]. The histidine tag was removed from recombinant proteins using thrombin before injection into rabbits. The purified recombinant protein was briefly reisolated by SDS-PAGE. The area of the gel containing the sample band was homogenized with 1 mL saline and mixed with 1 mL complete Freund's adjuvant. The thoroughly mixed samples were subcutaneously injected into the rabbits through a vein along the edge of the ear once per week for 3 weeks. Subsequently, approximately 200 μg highly purified recombinant protein was injected without adjuvant once weekly for 4 weeks through a vein along the edge of the ear. Blood samples were collected to perform western blot analysis after the last booster.

Western blotting was performed to test the quality of the abovementioned antibody. Briefly, the purified protein was loaded onto the gel of SDS-PAGE. The protein was then electrically transferred onto the nitrocellulose membrane, and bands were detected via immunoblotting assay as described in previous article [27].

### 2.8. Enzyme catalysis assay

The enzyme activity of r*Pc*-DDC was tested by the method described by zhou et al. in a previous article [6]. Briefly, 50 mL of r*Pc*-DDC (10 mg) was added into the reaction mixture, which was composed of 30 mmol $L^{-1}$ L-dopa and 0.4 mmol $L^{-1}$ pyridoxal phosphate (PLP) in 500 mL PBS. In addition, 50 mL of 1 × PBS dialysate served as the negative control reaction. The reaction was sustained for 1 h at 37 °C and then was terminated by cooling in an ice-water mixture. The amount of dopamine was tested by dopamine ELISA kit (USCNLIFE, USA) according to the manufacturer's protocol. Each assay was repeated three times for the subsequent statistical analysis. The enzymatic activity of r*Pc*-DDC was defined as the amount of dopamine (ng) produced by 1 mg r*Pc*-DDC in 1 h ($ng\, h^{-1} \cdot mg^{-1}$).

### 2.9. Mimetic hemocytes encapsulation assay in vitro

An *in vitro* mimetic hemocytes encapsulation assay was performed as described by zhou et al. with slight modifications [6]. Briefly, the renatured r*Pc*-DDC (200 μg $mL^{-1}$), BSA (200 μg $mL^{-1}$), and 1 × PBS were incubated with Ni-NTA agarose beads (Sangon, China), which were equilibrated in Tris-buffer saline (TBS, 20 mmol $L^{-1}$ Tris-HCl, 500 mmol $L^{-1}$ NaCl, 10 mmol $L^{-1}$ $CaCl_2$, pH 7.5) in a 1.5-mL tube with slow shaking at 4 °C overnight. Then, the protein-coated beads were washed with TBS buffer three times for 5 min each. The concentration of the beads was adjusted to approximately 180–200 beads per milliliter.

Hemolymph was extracted from the ventral sinus of normal crayfish using a 5-ml sterile syringe preloaded with 800 μl anticoagulant (10% sodium citrate, pH 7) [23]. Hemolymph was centrifuged immediately at 800 × *g* for 5 min (4 °C) to isolate hemocytes. The hemocytes were resuspended in 100 mL of Leibovitz $L^{-15}$ medium (Sigma, USA). Then, 3 mL of the hemocytes resuspended solution was added to each well of an agarose-coated 12-well cell culture plate (Sigma, USA). Subsequently, 1 mL of the protein-coated (or BSA, or 1 × PBS) agarose beads was added to the cell culture plate, and the plate was incubated at 28 °C for 6 h. The final results were observed under a microscope. Three parallel experiments were performed to confirm the results.

### 2.10. Microorganism binding assay

The microorganism binding assay of r*Pc*-DDC was carried out using a Gram-positive bacterium (*S. aureus*) and a Gram-negative bacterium (*E. ictaluri*). In brief, the overnight-cultured bacteria were pelleted by centrifugation at 6000 × *g* for 3 min, washed with TBS (10 mmol/l Tris-HCl, pH 7.5, 150 mmol/l NaCl), and thoroughly resuspended in TBS. The purified r*Pc*-DDC (0.2 mg/mL, 300 μl) in buffer A (50 mmol/l Tris-HCl, pH 8.0, 5 mmol/l EDTA) was incubated with 300 μl microorganisms ($2 \times 10^7$ cells/ml) while subjected to gentle rotation for 1 h at 37 °C. Subsequently, the microorganisms were pelleted, washed three times with TBS and subjected to elution with 7% SDS for 5 min. Finally, the bacterial cells were washed three times in 0.5 mL TBS. The washed bacteria were subjected to 12.5% SDS-PAGE. After SDS-PAGE was performed, western blot analysis was performed [27].

### 2.11. RNAi assay of Pc-ddc gene

*Pc-ddc* double strand RNA (dsRNA) was synthesized using the methods described previously in another article [19]. Crayfish were divided randomly into three groups (30 for each group), including *Pc*-DDC dsRNA (*dsPc-ddc*) injection group, GFP dsRNA (*dsGFP*) injection group, and normal group. Normal crayfish did not receive any treatment. *Pc*-DDC and GFP DNA fragments were amplified using *Pc*-DDC-Fi (5′-gcg taa tac gac tca cta tag gcg cga atg aac tag tgg acg-3′) and *Pc*-DDC-Ri (5′-gcg taa tac gac tca cta tag gcc tca aca cct cct ccc aag-3′) as well as GFP-Fi (5′-gcg taa tac gac tca cta tag gtg gtc cca att ctc gtg gaa c-3′) and GFP-Ri (5′-gcg taa tac gac tca cta tag gct tga agt tga cct tga tgc c-3′), respectively. The sequence of T7 promotor was underlined in the primers above. The DNA fragments obtained by PCR were used as templates for dsRNA synthesis. The dsRNA synthesis system (with a 50-μl total volume) was devised according to this following methods: 8 μg DNA templates, 20 μl 5 × transcription buffer, 2.4 μl A/U/C/GTP each (10 μM, TaKaRa, Japan), 60 U RNasin (TaKaRa, Japan), and 40 U T7 RNA polymerase (TaKaRa, Japan), mixed with RNase-Free water to a total volume 50 μl. After incubation at 37 °C for 4 h, the solution was added for a final volume of 100 μl with 20 μl 10 × DNase I buffer, 6 μl DNase I (TaKaRa, Japan) and 24 μl RNase-free water. In addition, then, the mixed solution was incubated again at 37 °C for 1 h in order to remove the DNA templates [23]. Subsequently, dsRNA was extracted with phenol/chloroform and precipitated with ethanol and then resuspended in 40 μl RNase-free water.

The prepared dsRNA (approximately 30 μg) was injected into the abdominal segment of each crayfish, and the second injection of dsRNA (approximately 30 μg) was given 24 h later to enhance the RNAi efficiency [19]. Then, the total RNA was isolated from the hemocytes of three groups of crayfish at 2 h after the second injection of dsRNA. Meanwhile, *S. aureus* or *E. ictaluri* ($2 \times 10^7$ cells per crayfish) was injected into the abdominal segment of each crayfish in each group [23]. Subsequently, the survival rates of crayfish in the three groups were counted at different time points (2, 6, 12, 24, 36, and 48 h) after bacterial injection. To evaluate the knockdown efficiency of *Pc-ddc*, qRT-PCR was performed using the primers *Pc-ddc*-RT-F (5′-gca gta gca aac tga ttc-3′) and *Pc-ddc*-RT-R (5′-gat agt tga gga gtt atc-3′). In addition, the crayfish of an additional group, which was injected with *S. aureus* or *E. ictaluri*, were used as a control. Three parallel experiments were carried out to increase the integrity of the experiments.

## 3. Results

### 3.1. Cloning of *Pc-ddc* cDNA

The *P. clarkii* hemocytes cDNA sample was used as the template for target gene PCR amplification. A 3693 bp intact cDNA sequence was obtained. After BLAST online analysis, it was nominated as *P. clarkii* dopa decarboxylase gene (*Pc-ddc*). The open reading frame (ORF) of *Pc-ddc* encoded 474 amino acids, which possessed a 377-amino-acid domain (Fig. 1) and a polyadenylation signal (aataaa) located 11 bp upstream of the polyA tail. The mature *Pc*-DDC (474 amino acids) had a predicted molecular mass of 52.99 kDa and an estimated *p*I of 5.98.

### 3.2. Multiple alignments and phylogenetic analysis

To study the amino acid sequence divergence of *Pc*-DDC with other DCC molecules, some invertebrate DDC molecules were chosen to perform sequence multiple alignments. According to the results of BLAST online analysis, *Aedes aegypti* DDC (XP001648264), *Antheraea pernyi* DDC (AAR23825), *Apis florae* DDC (XP003690125), *Drosophila melanogaster* DDC (NP724164), *Gryllus bimaculatus* DDC (BAJ83478), *Musca domestica* DDC (XP005179779), *Mythimna separate* DDC (BAB68549), *Papilio xuthus* DDC (BAE43825), *Spodoptera exigua* DDC (AFG25780), *Tenebrio molitor* DDC (BAA95568), *Tribolium castaneum* DDC (NP001096056), and *Zootermopsis nevadensis* DDC (KDR23678) were chosen for multiple alignments. The results showed that the sequence similarity was 81.9% among the abovementioned DDC molecules (Fig. 2). To further analyze the evolutionary relationship between *Pc*-DDC and other chosen invertebrate DDC molecules, phylogenetic analysis was performed. The results showed that only *Pc*-DDC was located in one branch of the evolutionary tree. Other chosen invertebrate DDC molecules are located in another branch of the evolutionary tree (Fig. 3).

### 3.3. Expression profile analysis of *Pc-ddc* in mRNA after bacterial challenge

To validate the roles of the *Pc-ddc* gene in the innate immune system of crayfish *in vivo*, tissue distribution and time course expression patterns after bacterial challenge were studied. In the research on *Pc-ddc* expression profiles, *18S RNA*, *β-actin*, and *GAPDH* genes were all used as internal controls. According to the qRT-PCR data, one of the best and the most stable genes will be chosen as the final candidate internal control. Finally, *18S RNA* was chosen as the internal control due to its high-quality repeatability. The results showed that *Pc-ddc* mRNA transcripts were mainly distributed in crayfish hemocytes, hepatopancreas, gills, and intestine (Fig. 4). In addition, the transcript of *Pc-ddc* was not found in the heart or stomach in the present detection methods. *Pc-ddc* was expressed at a relatively high level in hemocytes and gills. This protein was expressed at a relatively low level in the hepatopancreas and intestine.

After challenge with *S. aureus*, the expression level of *Pc-ddc* mRNA was clearly upregulated in the four tissues of crayfish. In the hemocytes, the expression level of *Pc-ddc* was clearly upregulated from 2 h to 12 h after bacterial challenge and reached the maximum level at 12 h (Fig. 5A). In the hepatopancreas, the expression level of *Pc-ddc* was clearly upregulated from 6 h to 36 h after bacterial challenge and reached the maximum level at 12 h (Fig. 5B). In the gills, the expression level of *Pc-ddc* was clearly upregulated from 6 h to 24 h after bacterial challenge and reached the maximum level at 12 h (Fig. 5C). In the intestine, the expression level of *Pc-ddc* was clearly upregulated from 6 h to 36 h after bacterial challenge and reached the maximum level at 24 h (Fig. 5D). The significant difference was analyzed for the abovementioned data.

After challenge with *E. ictaluri*, the expression level of *Pc-ddc* mRNA was also clearly upregulated in the four tissues of crayfish. In the hemocytes, the expression level of *Pc-ddc* was clearly upregulated from 2 h to 24 h after bacterial challenge and reached the maximum level at 24 h (Fig. 6A). In the hepatopancreas, the expression level of *Pc-ddc* was clearly upregulated from 2 h to 36 h after bacterial challenge and reached the maximum level at 12 h (Fig. 6B). In the gills, the expression level of *Pc-ddc* was clearly upregulated from 2 h to 24 h after bacterial challenge and reached the maximum level at 12 h (Fig. 6C). In the intestine, the expression level of *Pc-ddc* was clearly upregulated from 2 h to 24 h after bacterial challenge and reached the maximum level at 12 h (Fig. 6D). The significant difference was also analyzed for the abovementioned data.

### 3.4. Recombinant expression and purification

After induction by IPTG, r*Pc*-DDC was expressed in the *E. coli* recombinant expression system. The theoretically predicted molecular mass of r*Pc*-DDC was 58.59 kDa, which included the molecular mass of the His-tag. The SDS-PAGE results showed that the target band of r*Pc*-DDC was consistent with the theoretical value (Fig. 7). Then, r*Pc*-DDC was purified with His Bind resin chromatography.

After affinity purification, r*Pc*-DDC was used as a protein antigen to prepare polyclonal antibodies in rabbit. In the results of the western blot assay, the corresponding protein band (r*Pc*-DDC) was recognized by the polyclonal antibody produced by rabbit (Fig. 7).

### 3.5. Enzyme catalysis activity in vitro

After purification and dialysis by 1 × PBS, the concentration of the purified rPc-DDC was modulated and tested. The amount of dopamine was tested using a dopamine ELISA kit (USCNLIFE, USA) according to the manufacturer's protocol. The results showed that the enzyme

```
acaacgggagtaaggatggacgccgatcagttcagggcggcgtctaaggagatgacggag   60
                 M  D  A  D  Q  F  R  A  A  S  K  E  M  T  E   15
ttcatcgctagctacctgtccaacatcagagacaggcgagtgttgccagaggtggctccc  120
 F  I  A  S  Y  L  S  N  I  R  D  R  R  V  L  P  E  V  A  P   35
gggtacctgcgaccactgttgccaccacgggctcctgacacccctgacgagtggagcgat  180
 G  Y  L  R  P  L  L  P  P  R  A  P  D  T  P  D  E  W  S  D   55
gttatggctgatatagagagggtcatcatgcctgggggtaacacactggcactcccctcag  240
 V  M  A  D  I  E  R  V  I  M  P  G  V  T  H  W  H  S  P  Q   75
ttccacgcgtacttcccgacaggcaacagctacccggccatcttggccgacatgttgagt  300
 F  H  A  Y  F  P  T  G  N  S  Y  P  A  I  L  A  D  M  L  S   95
gacgccattggatgtatcggcttcacctggatatcatcaccggcctgcacggagctggag  360
 D  A  I  G  C  I  G  F  T  W  I  S  S  P  A  C  T  E  L  E  115
gtggttatgatggactggctcggccagcttatcggcctccctccacacttccttgcctcc  420
 V  V  M  M  D  W  L  G  Q  L  I  G  L  P  P  H  F  L  A  S  135
tcaggggggcaagggcggtggcgtcatacagtcgacagcaagtgaagcgacgctggtggcc  480
 S  G  G  K  G  G  G  V  I  Q  S  T  A  S  E  A  T  L  V  A  155
atgttgtcagctcgggccaagactctcaagcacctcaaggaaggtcatcctgacccagct  540
 M  L  S  A  R  A  K  T  L  K  H  L  K  E  G  H  P  D  P  A  175
gctagtgatgctctcaagctggtagcttatgcctcagaccaggcccactcgtccgtggag  600
 A  S  D  A  L  K  L  V  A  Y  A  S  D  Q  A  H  S  S  V  E  195
cgagcagggatgctggcgggggtgaagctgcaccaggtgacctcagatgacagcttcgcc  660
 R  A  G  M  L  A  G  V  K  L  H  Q  V  T  S  D  D  S  F  A  215
atgcgcggcgcagctctacgagaagcaattgtcaaggataaacagctcggactcattccg  720
 M  R  G  A  A  L  R  E  A  I  V  K  D  K  Q  L  G  L  I  P  235
tttttcgtggtgggcactgtcggagcaacaccagcctgttcgtttgacaacctgcgagag  780
 F  F  V  V  G  T  V  G  A  T  P  A  C  S  F  D  N  L  R  E  255
atcgggacggtggcgaaggaatttcatttatggcaccacgtcgacgccgcgtacgctggg  840
 I  G  T  V  A  K  E  F  H  L  W  H  H  V  D  A  A  Y  A  G  275
tcagcgatggtgtgtgaggagttccggtacctgatggacggggttgagctggccgacagc  900
 S  A  M  V  C  E  E  F  R  Y  L  M  D  G  V  E  L  A  D  S  295
ttcaacttcaaccctcacaagtggctcctcgtcaacttcgactgttctgccatgtggata  960
 F  N  F  N  P  H  K  W  L  L  V  N  F  D  C  S  A  M  W  I  315
aaggacgcgaatgaactagtggacgcgttcaacgtggaccctctctacctgaagcatgag 1020
 K  D  A  N  E  L  V  D  A  F  N  V  D  P  L  Y  L  K  H  E  335
aaccagggacagatgcctgactacaggcactggcagatacctctgggcggcgcttcagg 1080
 N  Q  G  Q  M  P  D  Y  R  H  W  Q  I  P  L  G  R  R  F  R  355
tctctcaaactgtggttcgtgatgaggatgtacggcagagttggtctccaggcacacatc 1140
 S  L  K  L  W  F  V  M  R  M  Y  G  R  V  G  L  Q  A  H  I  375
aggaagcaggtgggattggcgcaccagttcgagaaccatgttaagggcgactcaagattc 1200
 R  K  Q  V  G  L  A  H  Q  F  E  N  H  V  K  G  D  S  R  F  395
gagatcattctccccgtcactcttggcctcgtctgcttccgtcttaagagagacaacgag 1260
 E  I  I  L  P  V  T  L  G  L  V  C  F  R  L  K  R  D  N  E  415
gtcaacgaggcgctgctcaagaacctcaacgctggaggtgtcattcacctcgtcccttcc 1320
 V  N  E  A  L  L  K  N  L  N  A  G  G  V  I  H  L  V  P  S  435
aagatcaggagcacctatttcctcaggtttgctgtatgttcaagtatgatggagccgtat 1380
 K  I  R  S  T  Y  F  L  R  F  A  V  C  S  S  M  M  E  P  Y  455
gatgttgacaaggcttgggaggaggtgttgaggcagacggagatcattctgcaggagtaa 1440
 D  V  D  K  A  W  E  E  V  L  R  Q  T  E  I  I  L  Q  E  *  474
tgcctcccgcttttgcagtagcaaactgattcctctccaacaatccctccatcagaaata 1500
gattgttcatcaaccactcctcgagcagaaatagatcactacgtaaccactccacctgca 1560
gaaatagatcactccacaacgaatttaatagctgaaataatcactcctcaaccacttcac 1620
cagcagaaatagataactcctcaactatcctgccagctgaaatagatcactcctcaacta 1680
ccataccagccgaaatagatgactcctcgactaccatatgagctgaaatagatcactcct 1740
caactaccataccagctgaaatagatcactcctcaactaccataccagctgaaatagatc 1800
actcctcaactaccataccagctgaaatagatcactcctcaactaccataccagctgaaa 1860
tagatcactcctcaaccaccataccagctgaaattgatcactcagccacatgcaagagtg 1920
gaaatataaacattcttaaccatcacagtatcagatattgatcaatcctcaagcatccca 1980
ctagcacagtcatcactcatctatccaaggttgtagggattgggccttccaatccgaata 2040
tgggcagccacaaccatccaggtagtagtgatggctggcttgactaagatagactttttt 2100
ttaagccttccctttcaagattttgttttgtttacacctgtgcacaagcgaagccatcca 2160
gagaccgtcgcgaacgtacacaacacaccagcggatgcaagacattaaatgaacttaatt 2220
attgctggtagtcaagaaaatatgaaaaaaaatgtcatatgcataggctatctttgttta 2280
tgtattgtgattttgttttcaagaatatgtatggctatcagttataatagacgtataaca 2340
gtatcagtagtagtagcaatggttgtagtggtagtggtagtagcagacgcagaagtataa 2400
taatggtattattataccaaaacagttcacacatttctaaacatactaacagtcctacg 2460
ttaatgtttaggcttttcaatcctatgcatttctcatctttcagtcaaataacaatgcta 2520
ttatttaataaatatttattatatttcttcctgaaggtttttccagttgttccagcaat 2580
gttcacctgtccagacttttgagtgcttcagtcttccaggatttatgttacataaatgcc 2640
agtatggcagctggaagatctggaagtgccttcatttttgttctaggctcgagtataata 2700
atttaaaatcaagtgttagtgactaaatcatcatatgagaactatgaaacatggttaaat 2760
gattatttttacaccatctctcacacctgaaaatgtaggtagggagtggcgaggcttcgg 2820
aactttatcctttcttatttctaaagtatcggttaatgtgttggagccagccacggtat 2880
tattatttactttctctatattaattaatcttaacagctagatatttgatagcagacaaa 2940
tgaattcattggataagagcagagaagaatatttttaaatcatagatctgaaattaaatt 3000
aaaaactcattaatgaattgttaaacatattaaccattaacttatctaccacaatcacga 3060
aaataacagataattaagaggaacgatacacagggtacttagttatcatcacagccgtgg 3120
gctcaaggcctagtcaagactgtcataataaggttgaattactgaccctgcccaggatgc 3180
aaatccacaacaagctgactaactcttgggtacctatttactgctaggtggacatgggta 3240
ttaggtgataggaaattcccccaattatttctgtcccgcctgggattcgaacccggaatt 3300
ctagattgtgagttgagaatgaaccctactctactgcagggatccttaagtctactcaaa 3360
ttaagtctactgaatattcagatttattttcaactaaaaatgccaatcatggccaattca 3420
aactgaagtaccattccctgcttccctaagtatatagtatattatatatttcattcaccg 3480
tcccagtagcctcatcaattttatgttttgatacaagatgatatgatgctcccagtgtaa 3540
cgtctgtacttaagggaacaccagataagtgcctccagtgctcggtgagtgtgtgtgcgc 3600
ttccctacatgcactcactaaaacagcacccctattgttatgaaataaaatggatcaatg 3660
aaaaaaaagaaaaaaaaaaaaaaaaaaaaaaaa                            3693
```

**Fig. 1.** Nucleotide sequence of *Pc-ddc* cDNA and the deduced amino acid sequence. The structural domain is underlined. The polyadenylation signal (aataaa) is shown in italic.

catalysis activity of r*Pc*-DDC was 35 ± 2.8 ng h$^{-1}$ mg$^{-1}$ (n = 3). In other words, 35 ± 2.8 ng dopamine was catalyzed to produce 1 mg r*Pc*-DDC in 1 h.

### 3.6. Hemocytes encapsulation function

Mimetic hemocytes encapsulation was detected by an encapsulation assay *in vitro*. After coating with r*Pc*-DDC, BSA, and 1 × PBS, the agarose beads were incubated with crayfish hemocytes at 28 °C for 6 h. The final results observed by microscopy showed that the encapsulation rate of beads coated with r*Pc*-DDC was clearly increased (Fig. 8B) compared with the encapsulation rate of beads coated with 1 × PBS (Fig. 8A) or BSA (Fig. 8C).

### 3.7. Bacterial binding activity of r*Pc*-DDC

To further study the potential antibacterial innate immune roles of r*Pc*-DDC, a bacterial binding assay was performed. The results showed that r*Pc*-DDC could strongly bind to *S. aureus* and *E. ictaluri* (Fig. 9), which implied that r*Pc*-DDC may play a crucial role in the innate immune response to bacteria.

### 3.8. Involvement of *Pc-ddc* in the antibacterial innate immune of crayfish

The RNAi assay was performed to validate the role of *Pc-ddc* in crayfish antibacterial innate immunity. Two hours after the second dsRNA injection, total RNA was isolated from the hemocytes of three groups of crayfish to detect the target gene's expression level. The results showed that *Pc-ddc* was successfully knocked down compared with the other two groups (Fig. 10A). Subsequently, *S. aureus* and *E. ictaluri* were injected into the crayfish abdominal segment of three groups to count the number of survival crayfish at different time points (0, 6, 12, 24, 36, and 48 h) after the bacteria were injected. Additionally, the crayfish of an additional group, which was injected *S. aureus* or *E. ictaluri*, was used as a control. The results showed that when *Pc-ddc* was knocked down, the number of surviving crayfish clearly decreased after *S. aureus* was injected compared with other groups (Fig. 10B). Additionally, when *Pc-ddc* was knocked down, the number of surviving crayfish was also clearly decreased after infection by *E. ictaluri* compared with other groups (Fig. 10C). These results indicated that endogenous *Pc-ddc* was related to the antibacterial innate immunity of crayfish.

## 4. Discussion

Accumulating evidence indicates that endogenous monoamines, primarily including dopamine and serotonin, act as important neurotransmitters or neuromodulators in the nervous system of vertebrates and invertebrates [29]. In the dopaminergic signaling pathway, dopamine is synthesized from L-dopa by DDC. Serotonin is also synthesized by DDC from 5-hydroxy-L-tryptophan [30]. Recent findings have indicated that DDC may play an important role in the immunomodulation process. In the present study, a new *ddc* gene was identified from *P. clarkii* hemocytes, which was known as *Pc-ddc*. The full-length cDNA

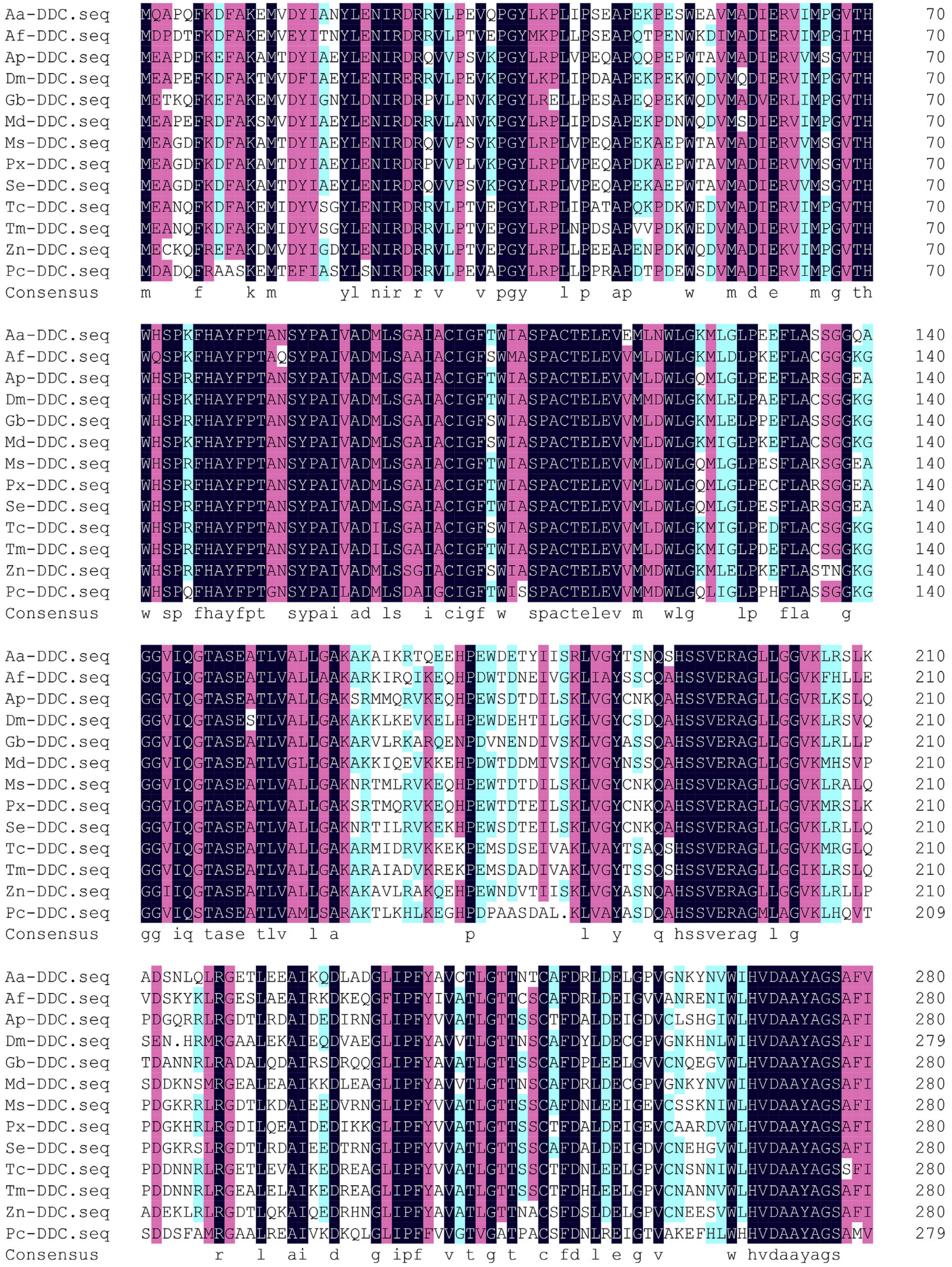

```
Aa-DDC.seq   MQAPQFKDFAKEMVDYIANYLENIRDRRVLPEVQPGYLKPLIPSEAPEKPESWEAVMADIERVIMPGVTH    70
Af-DDC.seq   MDPDTFKDFAKEMVEYITNYLENIRDRRVLPTVEPGYMKPLLPSEAPQTPENWKDIMADIERVIMPGITH    70
Ap-DDC.seq   MEAPDFKEFAKAMTDYIAEYLENIRDRQVVPSVKPGYLRPLVPEQAPQQPEPWTAVMADIERVVMSGVTH    70
Dm-DDC.seq   MEAPEFKDFAKTMVDFIAEYLENIRERRVLPEVKPGYLKPLIPDAAPEKPEKWQDVMQDIERVIMPGVTH    70
Gb-DDC.seq   METKQFKEFAKEMVDYIGNYLDNIRDRPVLPNVKPGYLRELLPESAPEQPEKWQDVMADVERLIMPGVTH    70
Md-DDC.seq   MEAPEFRDFAKSMVDYIAEYLENIRDRRVLANVKPGYLRPLIPDSAPEKPDNWQDVMSDIERVIMPGVTH    70
Ms-DDC.seq   MEAGDFKDFAKAMTDYIAEYLENIRDRQVVPSVKPGYLRPLVPEQAPEKAEPWTAVMADIERVVMSGVTH    70
Px-DDC.seq   MEAGDFKDFAKAMTDYIAEYLENIRDRPVVPLVKPGYLRPLVPEQAPDKAEPWTAVMADIERVVMSGVTH    70
Se-DDC.seq   MEAGDFKDFAKAMTDYIAEYLENIRDRQVVPSVKPGYLRPLVPEQAPEKAEPWTAVMADIERVVMSGVTH    70
Tc-DDC.seq   MEANQFKDFAKEMIDYVSGYLENIRDRRVLPTVEPGYLRPLIPATAPQKPDKWEDVMADIERVIMPGVTH    70
Tm-DDC.seq   MEANQFKDFAKEMIDYVSGYLENIRDRRVLPTVEPGYLRPLNPDSAPVVPDKWEDVMADIERVIMPGVTH    70
Zn-DDC.seq   MECKQFREFAKDMVDYIGDYLENIRDRRVLPTVEPGYLRPLLPEEAPENPDKWQDVMADIEKVIMPGVTH    70
Pc-DDC.seq   MDADQFRAASKEMTEFIASYLSNIRDRRVLPEVAPGYLRPLLPPRAPDTPDEWSDVMADIERVIMPGVTH    70
Consensus    m    f    k m      yl nir r v   v pgy   l p  ap     w   m d e   m g th

Aa-DDC.seq   WHSPKFHAYFPTANSYPAIVADMLSGAIACIGFTWIASPACTELEVEMLNWLGKMLGLPEEFLASSGGQA   140
Af-DDC.seq   WQSPKFHAYFPTAQSYPAIVADMLSAAIACIGFSWMASPACTELEVVMLDWLGKMLDLPKEFLACGGGKG   140
Ap-DDC.seq   WHSPRFHAYFPTANSYPAIVADMLSGAIACIGFTWIASPACTELEVVMLDWLGQMLGLPEEFLARSGGEA   140
Dm-DDC.seq   WHSPKFHAYFPTANSYPAIVADMLSGAIACIGFTWIASPACTELEVVMMDWLGKMLELPAEFLACSGGKG   140
Gb-DDC.seq   WHSPRFHAYFPTANSYPAIVADMLSGAIACIGFSWIASPACTELEVVMLDWLGKMLELPPEFLASSGGKG   140
Md-DDC.seq   WHSPKFHAYFPTANSYPAIVADMLSGAIACIGFSWIASPACTELEVVMLDWLGKMIGLPKEFLACSGGKG   140
Ms-DDC.seq   WHSPRFHAYFPTANSYPAIVADMLSGAIACIGFTWIASPACTELEVVMLDWLGQMLGLPESFLARSGGEA   140
Px-DDC.seq   WHSPRFHAYFPTANSYPAIVADMLSGAIACIGFTWIASPACTELEVVMLDWLGQMLGLPECFLARSGGEA   140
Se-DDC.seq   WHSPRFHAYFPTANSYPAIVADMLSGAIACIGFTWIASPACTELEVVMLDWLGQMLGLPESFLARSGGEA   140
Tc-DDC.seq   WHSPRFHAYFPTANSYPAIVADILSGAIACIGFSWIASPACTELEVVMLDWLGKMIGLPEDFLACSGGKG   140
Tm-DDC.seq   WHSPRFHAYFPTANSYPAIVADILSGAIACIGFTWIASPACTELEVVMLDWLGKMIGLPDEFLACSGGKG   140
Zn-DDC.seq   WHSPRFHAYFPTANSYPAIVADMLSSGIACIGFSWIASPACTELEVVMMDWLGKMLELPKEFLASTNGKG   140
Pc-DDC.seq   WHSPQFHAYFPTGNSYPAILADMLSDAIGCIGFTWISSPACTELEVVMMDWLGQLIGLPPHFLASSGGKG   140
Consensus    w sp fhayfpt  sypai ad ls  i cigf w  spactelev m  wlg    lp  fla   g

Aa-DDC.seq   GGVIQGTASEATLVALLGAKAKAIKRTQEEHPEWDETYIISRLVGYTSNQSHSSVERAGLLGGVKLRSLK   210
Af-DDC.seq   GGVIQGTASEATLVALLAAKARKIRQIKEQHPDWTDNEIVGKLIAYSSCQAHSSVERAGLLGGVKFHLLE   210
Ap-DDC.seq   GGVIQGTASEATLVALLGAKSRMMQRVKEQHPEWSDTDILSKLVGYCNKQAHSSVERAGLLGGVRLKSLQ   210
Dm-DDC.seq   GGVIQGTASESTLVALLGAKAKKLKEVKELHPEWDEHTILGKLVGYCSDQAHSSVERAGLLGGVKLRSVQ   210
Gb-DDC.seq   GGVIQGTASEATLVALLGAKARVLRKARQENPDVNENDIVSKLVGYASSQAHSSVERAGLLGGVKLRLLP   210
Md-DDC.seq   GGVIQGTASEATLVGLLGAKAKKIQEVKKEHPDWTDDMIVSKLVGYNSSQAHSSVERAGLLGGVKMHSVP   210
Ms-DDC.seq   GGVIQGTASEATLVALLGAKNRTMLRVKEQHPEWTDTDILSKLVGYCNKQAHSSVERAGLLGGVKLRALQ   210
Px-DDC.seq   GGVIQGTASEATLVALLGAKSRTMQRVKEQHPEWTDTEILSKLVGYCNKQAHSSVERAGLLGGVKMRSLK   210
Se-DDC.seq   GGVIQGTASEATLVALLGAKNRTILRVKEKHPEWSDTEILSKLVGYCNKQAHSSVERAGLLGGVKLRLLQ   210
Tc-DDC.seq   GGVIQGTASEATLVALLGAKARMIDRVKKEKPEMSDSEIVAKLVAYTSAQSHSSVERAGLLGGVKMRGLQ   210
Tm-DDC.seq   GGVIQGTASEATLVALLGAKARAIADVKREKPEMSDADIVAKLVGYTSSQSHSSVERAGLLGGIKLRSLQ   210
Zn-DDC.seq   GGIIQGTASEATLVALLGAKAKAVLRAKQEHPEWNDVTIISKLVGYASNQAHSSVERAGLLGGVKLRLLP   210
Pc-DDC.seq   GGVIQSTASEATLVAMLSARAKTLKHLKEGHPDPAASDAL.KLVAYASDQAHSSVERAGMLAGVKLHQVT   209
Consensus    gg iq tase tlv  l a            p          l  y   q hssverag l g

Aa-DDC.seq   ADSNLQLRGETLEEAIKQDLADGLIPFYAVCTLGTTNTCAFDRLDELGPVGNKYNVWIHVDAAYAGSAFV   280
Af-DDC.seq   VDSKYKLRGESLAEAIRKDKEQGFIPFYIVATLGTTCSCAFDRLDEIGVVANRENIWLHVDAAYAGSAFI   280
Ap-DDC.seq   PDGQRRLRGDTLRDAIDEDIRNGLIPFYVVATLGTTSSCTFDALDEIGDVCLSHGIWLHVDAAYAGSAFI   280
Dm-DDC.seq   SEN.HRMRGAALEKAIEQDVAEGLIPFYAVVTLGTTNSCAFDYLDECGPVGNKHNLWIHVDAAYAGSAFI   279
Gb-DDC.seq   TDANNRLRADALQDAIRSDRQQGLIPFYAVATLGTTSSCAFDPLEELGVVCNQEGVWLHVDAAYAGSAFI   280
Md-DDC.seq   SDDKNSMRGEALEAAIKKDLEAGLIPFYAVVTLGTTNSCAFDRLDECGPVGNKYNVWIHVDAAYAGSAFI   280
Ms-DDC.seq   PDGKRRLRGDTLKDAIEEDVRNGLIPFYVVATLGTTSSCAFDNLEEIGEVCSSKNIWLHVDAAYAGSAFI   280
Px-DDC.seq   PDGKHRLRGDILQEAIDEDIKKGLIPFYVVATLGTTSSCTFDALDEIGEVCAARDVWLHVDAAYAGSAFI   280
Se-DDC.seq   PDGKRSLRGDTLRDAIEEDTRNGLIPFYVVATLGTTSSCAFDALDEIGDVCNEHGVWLHVDAAYAGSAFI   280
Tc-DDC.seq   PDDNNRLRGETLEVAIKEDREAGLIPFYVVATLGTTSSCTFDNLEELGPVCNSNNIWLHVDAAYAGSSFI   280
Tm-DDC.seq   PDDNNRLRGEALELAIKEDREAGLIPFYAVATLGTTSSCTFDHLEELGPVCNANNVWLHVDAAYAGSAFI   280
Zn-DDC.seq   ADEKLRLRGDTLQKAIQEDRHNGLIPFYAVATLGTTNACSFDSLDELGPVCNEESVWLHVDAAYAGSAFI   280
Pc-DDC.seq   SDDSFAMRGAALREAIVKDKQLGLIPFFVVGTVGATPACSFDNLREIGTVAKEFHLWHHVDAAYAGSAMV   279
Consensus           r   l  ai  d   g ipf  v t g t  c fd l e g v      w hvdaayags
```

**Fig. 2.** Multiple alignments of DDC proteins including *A. aegypti* DDC (XP001648264), *A. pernyi* DDC (AAR23825), *A. florae* DDC (XP003690125), *D. melanogaster* DDC (NP724164), *G. bimaculatus* DDC (BAJ83478), *M. domestica* DDC (XP005179779), *M. separate* DDC (BAB68549), *P. xuthus* DDC (BAE43825), *S. exigua* DDC (AFG25780), *T. molitor* DDC (BAA95568), *T. castaneum* DDC (NP001096056), *Z. nevadensis* DDC (KDR23678). The numbers on the right indicate the amino acid position of different sequences. Different colors represent the different conservations of amino acids. (For interpretation of the references to color in this figure legend, the reader is referred to the Web version of this article.)

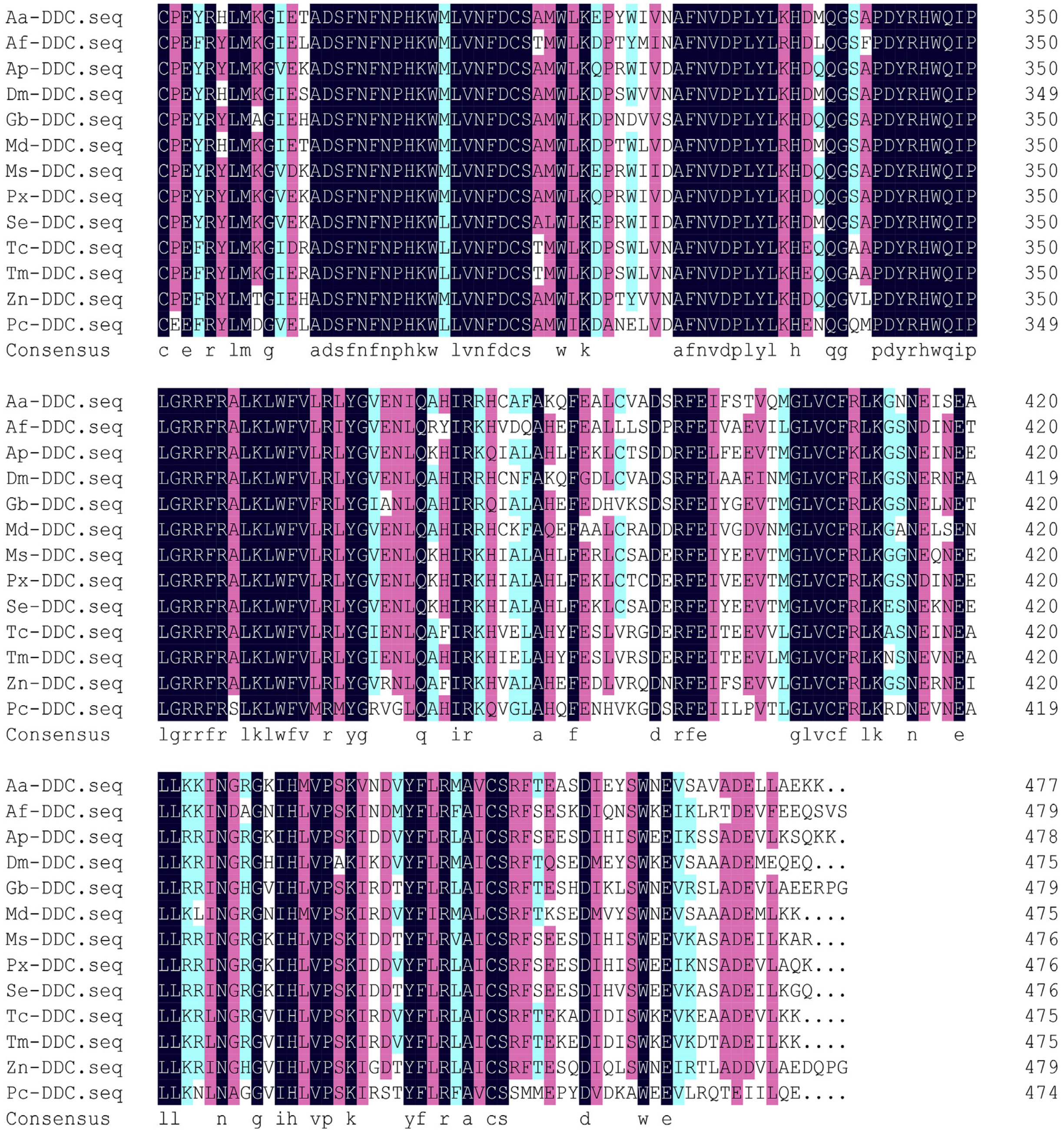

```
Aa-DDC.seq   CPEYRHLMKGIETADSFNFNPHKWMLVNFDCSAMWLKEPYWIVNAFNVDPLYLKHDMQGSAPDYRHWQIP   350
Af-DDC.seq   CPEFRYLMKGIELADSFNFNPHKWMLVNFDCSTMWLKDPTYMINAFNVDPLYLRHDLQGSFPDYRHWQIP   350
Ap-DDC.seq   CPEYRYLMKGVEKADSFNFNPHKWMLVNFDCSAMWLKQPRWIVDAFNVDPLYLKHDQQGSAPDYRHWQIP   350
Dm-DDC.seq   CPEYRHLMKGIESADSFNFNPHKWMLVNFDCSAMWLKDPSWVVNAFNVDPLYLKHDMQGSAPDYRHWQIP   349
Gb-DDC.seq   CPEYRYLMAGIEHADSFNFNPHKWMLVNFDCSAMWLKDPNDVVSAFNVDPLYLKHDQQGSAPDYRHWQIP   350
Md-DDC.seq   CPEYRHLMKGIETADSFNFNPHKWMLVNFDCSAMWLKDPTWLVDAFNVDPLYLRHDMQGSAPDYRHWQIP   350
Ms-DDC.seq   CPEYRYLMKGVDKADSFNFNPHKWMLVNFDCSAMWLKEPRWIIDAFNVDPLYLKHDQQGSAPDYRHWQIP   350
Px-DDC.seq   CPEYRYLMKGVEKADSFNFNPHKWMLVNFDCSAMWLKQPRWIVDAFNVDPLYLKHDQQGSAPDYRHWQIP   350
Se-DDC.seq   CPEYRYLMKGVEKADSFNFNPHKWLLVNFDCSALWLKEPRWIIDAFNVDPLYLKHDMQGSAPDYRHWQIP   350
Tc-DDC.seq   CPEFRYLMKGIDRADSFNFNPHKWLLVNFDCSTMWLKDPSWLVNAFNVDPLYLKHEQQGAAPDYRHWQIP   350
Tm-DDC.seq   CPEFRYLMKGIERADSFNFNPHKWLLVNFDCSTMWLKDPSWLVNAFNVDPLYLKHEQQGAAPDYRHWQIP   350
Zn-DDC.seq   CPEFRYLMTGIEHADSFNFNPHKWMLVNFDCSAMWLKDPTYVVNAFNVDPLYLKHDQQGVLPDYRHWQIP   350
Pc-DDC.seq   CEEFRYLMDGVELADSFNFNPHKWLLVNFDCSAMWIKDANELVDAFNVDPLYLKHENQGQMPDYRHWQIP   349
Consensus    c e r lm g   adsfnfnphkw lvnfdcs  w k       afnvdplyl h  qg  pdyrhwqip

Aa-DDC.seq   LGRRFRALKLWFVLRLYGVENIQAHIRRHCAFAKQFEALCVADSRFEIFSTVQMGLVCFRLKGNNEISEA   420
Af-DDC.seq   LGRRFRALKLWFVLRIYGVENLQRYIRKHVDQAHEFEALLLSDPRFEIVAEVILGLVCFRLKGSNDINET   420
Ap-DDC.seq   LGRRFRALKLWFVLRLYGVENLQKHIRKQIALAHLFEKLCTSDDRFELFEEVTMGLVCFKLKGSNEINEE   420
Dm-DDC.seq   LGRRFRALKLWFVLRLYGVENLQAHIRRHCNFAKQFGDLCVADSRFELAAEINMGLVCFRLKGSNERNEA   419
Gb-DDC.seq   LGRRFRALKLWFVFRLYGIANLQAHIRRQIALAHEFEDHVKSDSRFEIYGEVTMGLVCFRLKGSNELNET   420
Md-DDC.seq   LGRRFRALKLWFVLRLYGVENLQAHIRRHCKFAQEFAALCRADDRFEIVGDVNMGLVCFRLKGANELSEN   420
Ms-DDC.seq   LGRRFRALKLWFVLRLYGVENLQKHIRKHIALAHLFERLCSADERFEIYEEVTMGLVCFRLKGGNEQNEE   420
Px-DDC.seq   LGRRFRALKLWFVLRLYGVENLQKHIRKHIALAHLFEKLCTCDERFEIVEEVTMGLVCFRLKGSNDINEE   420
Se-DDC.seq   LGRRFRALKLWFVLRLYGVENLQKHIRKHIALAHLFEKLCSADERFEIYEEVTMGLVCFRLKESNEKNEE   420
Tc-DDC.seq   LGRRFRALKLWFVLRLYGIENLQAFIRKHVELAHYFESLVRGDERFEITEEVVLGLVCFRLKASNEINEA   420
Tm-DDC.seq   LGRRFRALKLWFVLRLYGIENLQAHIRKHIELAHYFESLVRSDERFEITEEVLMGLVCFRLKNSNEVNEA   420
Zn-DDC.seq   LGRRFRALKLWFVLRLYGVRNLQAFIRKHVALAHEFEDLVRQDNRFEIFSEVVLGLVCFRLKGSNERNEI   420
Pc-DDC.seq   LGRRFRSLKLWFVMRMYGRVGLQAHIRKQVGLAHQFENHVKGDSRFEIILPVTLGLVCFRLKRDNEVNEA   419
Consensus    lgrrfr lklwfv r yg    q  ir     a  f      d rfe       glvcf lk  n   e

Aa-DDC.seq   LLKKINGRGKIHMVPSKVNDVYFLRMAVCSRFTEASDIEYSWNEVSAVADELLAEKK..              477
Af-DDC.seq   LLKKINDAGNIHLVPSKINDMYFLRFAICSRFSESKDIQNSWKEIKLRTDEVFEEQSVS              479
Ap-DDC.seq   LLRRINGRGKIHLVPSKIDDVYFLRLAICSRFSEESDIHISWEEIKSSADEVLKSQKK.              478
Dm-DDC.seq   LLKRINGRGHIHLVPAKIKDVYFLRMAICSRFTQSEDMEYSWKEVSAAADEMEQEQ...              475
Gb-DDC.seq   LLRRINGHGVIHLVPSKIRDTYFLRLAICSRFTESHDIKLSWNEVRSLADEVLAEERPG              479
Md-DDC.seq   LLKLINGRGNIHMVPSKIRDVYFIRMALCSRFTKSEDMVYSWNEVSAAADEMLKK....              475
Ms-DDC.seq   LLRRINGRGKIHLVPSKIDDTYFLRVAICSRFSEESDIHISWEEVKASADEILKAR...              476
Px-DDC.seq   LLRRINGRGKIHLVPSKIDDVYFLRLAICSRFSEESDIHISWEEIKNSADEVLAQK...              476
Se-DDC.seq   LLRRINGRGKIHLVPSKIDDTYFLRLAICSRFSEESDIHVSWEEVKASADEILKGQ...              476
Tc-DDC.seq   LLKRLNGRGVIHLVPSKIRDVYFLRLAICSRFTEKADIDISWKEVKEAADEVLKK....              475
Tm-DDC.seq   LLKRLNGRGVIHLVPSKIRDVYFLRLAICSRFTEKEDIDISWKEVKDTADEILKK....              475
Zn-DDC.seq   LLKRINGHGVIHLVPSKIGDTYFLRLAICSRFTESQDIQLSWNEIRTLADDVLAEDQPG              479
Pc-DDC.seq   LLKNLNAGGVIHLVPSKIRSTYFLRFAVCSSMMEPYDVDKAWEEVLRQTEIILQE....              474
Consensus    ll   n  g ih vp k    yf r a cs      d    w e
```

**Fig. 2.** (*continued*)

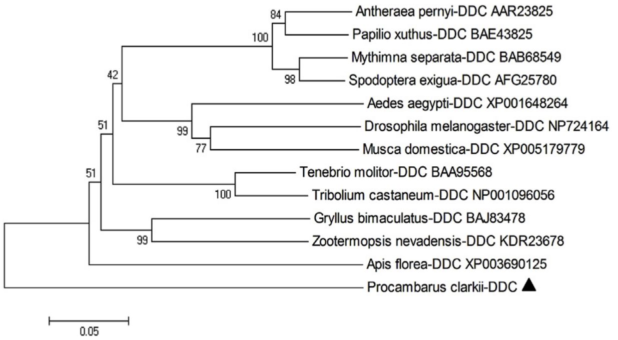

**Fig. 3.** Phylogenetic analysis of *Pc*-DDC with other chosen DDC proteins. NJ tree was produced with the MEGA 7.0 software. One thousand bootstraps were carried out to check the repeatability of the result.

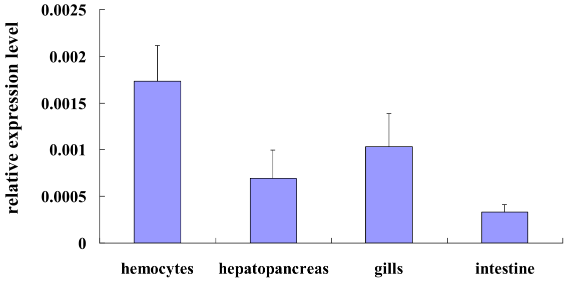

**Fig. 4.** Expression pattern analysis of *Pc-ddc* in different tissues including hemocytes, hepatopancreas, gills, and intestine of non-challenged crayfish. *18S RNA* was used as inner control.

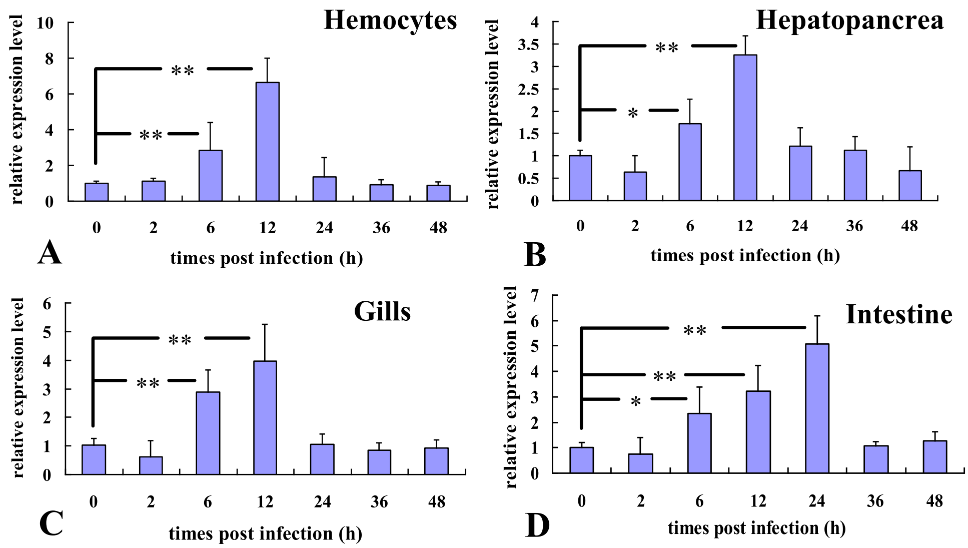

**Fig. 5.** Time course expression patterns of *Pc-ddc* analyzed by qRT-PCR. (A), (B), (C), and (D) stand for expression profiles in hemocytes, hepatopancreas, gills, and intestine at different timepoints after *S. aureus* challenge. *18S RNA* was used as a control. The histograms below show the statistical analysis of the qRT-PCR results. Data were expressed as the ratio of *Pc-ddc* to *18S RNA* mRNA.The asterisks indicate significant differences (*: P < 0.05, **: P < 0.01) from the control. Error bars represent ± SD of 3 independent PCR amplifications and quantifications.

sequence of *Pc-ddc* was obtained after the gene cloning experiment. The amino acid sequence alignment and phylogenetic analysis were performed. The results indicated that *Pc*-DDC might be a new member of the DDC family in invertebrates, which probably possessed new functions.

To date, the functions of DDC have been well-studied in different tissues of mammals. For example, immunoreactive structures of DDC were studied in the human midbrain, pons, and medulla [31]. In rats, the correlation between a time-dependent change in blood pressure and renal DDC activity was found after surgery for renal mass ablation [32]. In pigs, a nonneuronal DDC isoform was identified in the developing porcine brain [33]. The different roles of DDC have also been studied in the rhesus monkey brain [34], human kidney [35], rat liver [36], and human pulmonary carcinoid [37]. In addition, DDC was also found to be involved in the hypothalamus-pituitary-adrenocortical system, sympathetic nervous system, and immunity system to adjust the immune responses against various pathogens [38,39]. In invertebrates, DDC also plays an important role in the innate immune system. In *Penaeus monodon* and *Macrobrachium rosenbergii*, dopamine catalyzed by DDC had an effect on the host immunity and susceptibility to bacteria [40,41]. To validate the possible function of *Pc*-DDC in the NEI system of crayfish, the expression patterns of *Pc-ddc* mRNA transcript were

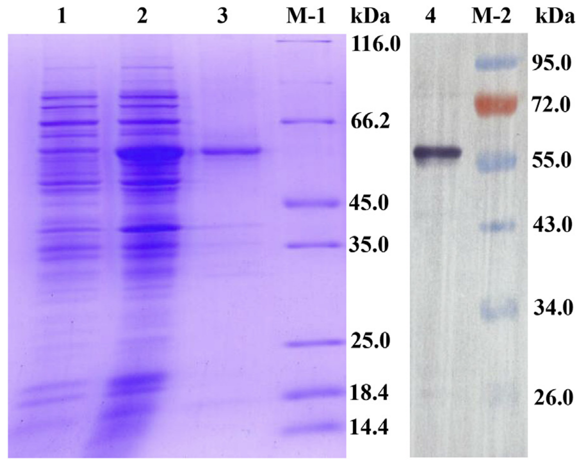

**Fig. 7.** SDS-PAGE analysis of the recombinant expression of *Pc*-DDC in *E. coli*. Lane 1, total proteins of *E. coli* without induction; lane 2, induction with IPTG; lane 3, purified recombinant protein; lane 4, western blot band recognized by corresponding antibody; and lane M − 1 and M − 2, standard protein markers.

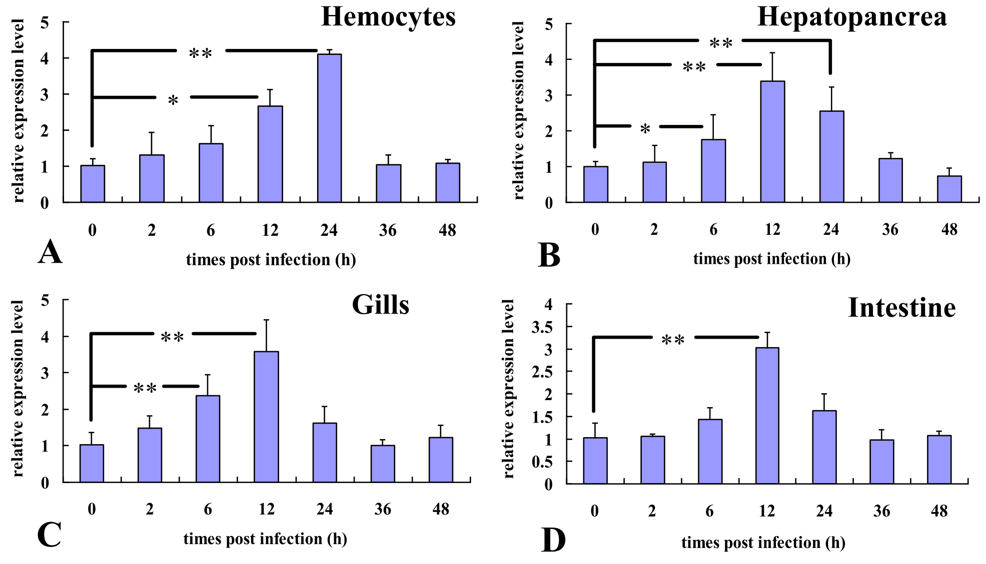

**Fig. 6.** Time course expression patterns of *Pc-ddc* analyzed by qRT-PCR. (A), (B), (C), and (D) stand for expression profiles in hemocytes, hepatopancreas, gills, and intestine at different timepoints after *E. ictaluri* challenge. *18S RNA* was used as a control. The histograms below show the statistical analysis of the qRT-PCR results. Data were expressed as the ratio of *Pc-ddc* to *18S RNA* mRNA.The asterisks indicate significant differences (*: P < 0.05, **: P < 0.01) from the control. Error bars represent ± SD of 3 independent PCR amplifications and quantifications.

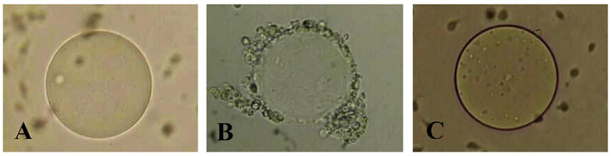

**Fig. 8.** The hemocytes encapsulation promoted by r*Pc*-DDC. Agarose beads coated with 1 × PBS (A), r*Pc*-DDC (B) and BSA (C).

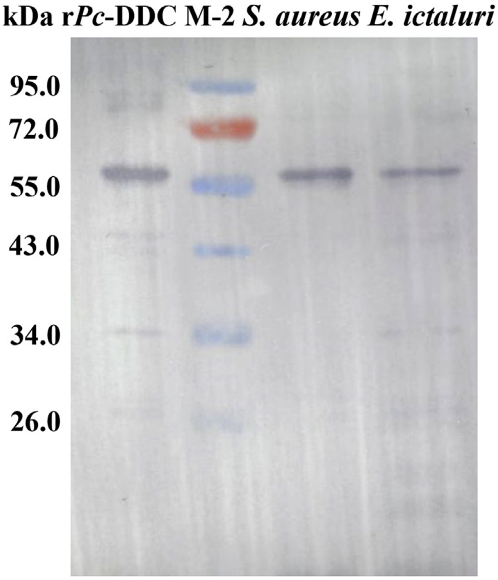

**Fig. 9.** Direct binding assay of r*Pc*-DDC to bacteria. The microorganism binding assay of r*Pc*-DDC was carried out using a Gram-positive bacterium (*S. aureus*) and a Gram-negative bacterium (*E. ictaluri*). The protein bands were recognized by the antiserum against r*Pc*-DDC in western bolt.

detected by qRT-PCR. The results showed that *Pc-ddc* mRNA transcripts were primarily distributed in crayfish hemocytes, hepatopancreas, gills, and intestine (Fig. 4). The expression level of *Pc-ddc* mRNA was clearly upregulated in hemocytes, hepatopancreas, gills, and intestine tissues of crayfish after challenge with *S. aureus* (Fig. 5) or *E. ictaluri* (Fig. 6). These results implied that *Pc-ddc* is likely to be involved in the immune defense against bacterial invasion.

To further study the functions of *Pc*-DDC in the crayfish innate immune system, in enzyme catalysis activity *in vitro*, and in promoting hemocytes encapsulation, the bacterial binding activity of r*Pc*-DDC was detected. The results of the enzyme catalysis assay showed that the enzyme activity of r*Pc*-DDC was 35 ± 2.8 ng $h^{-1}$ $mg^{-1}$ (n = 3). In other words, 35 ± 2.8 ng dopamine was catalyzed to produce 1 mg r*Pc*-DDC in 1 h. This result strongly proved that r*Pc*-DDC is a kind of dopa decarboxylase. In addition, the results of the mimetic crayfish hemocytes encapsulation assay showed that the encapsulation rate of beads coated with r*Pc*-DDC was clearly increased (Fig. 8B). The results of the bacterial binding assay showed that r*Pc*-DDC could strongly bind to *S. aureus* and *E. ictaluri* (Fig. 9). Because the binding bacteria activity was a key factor for the achievement of antibacterial function, it was reasonable to speculate that r*Pc*-DDC played an important role in defending against bacterial infection.

To validate the role of endogenous *Pc-ddc* in crayfish antibacterial innate immunity, an RNAi assay was performed. After *Pc-ddc* was knocked down (Fig. 10A), the number of surviving crayfish was clearly decreased after *S. aureus* was injected (Fig. 10B). The number of surviving crayfish was also clearly decreased after infection by *E. ictaluri* (Fig. 10C) when *Pc-ddc* was knocked down. These results indicated that endogenous *Pc-ddc* was associated with the antibacterial innate immunity of crayfish. We speculated that the synthesis of endogenous dopamine in crayfish was reduced after *Pc-ddc* was knocked down. Then, the dopamine signaling pathway was restrained. In particular, the production of melanin was inhibited. Subsequently, the crayfish mortality was increased.

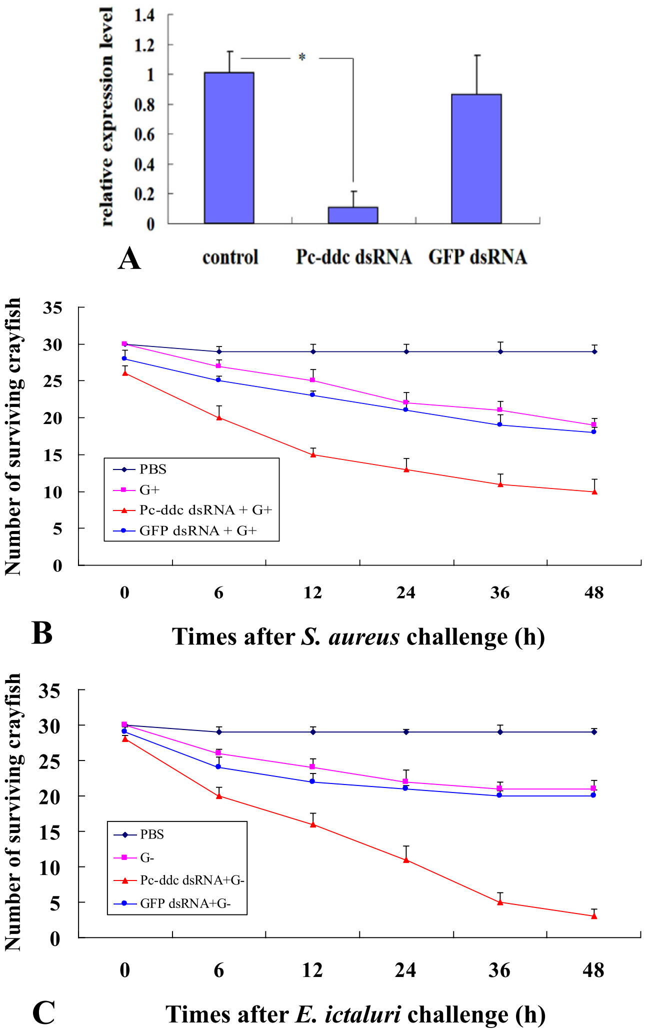

**Fig. 10.** RNAi assay was carried out to identify the role of *Pc-ddc* in crayfish antibacterial innate immunity. (A) qPCR indicated that injection dsRNA against *Pc-ddc* could obviously knock down the transcription of *Pc-ddc* in hemocytes of crayfish. 18sRNA was used as inner control. (B) Knockdown of *Pc-ddc* could obviously decrease the surviving rate of crayfish after challenged by *S. aureus*. (C) Knockdown of *Pc-ddc* could obviously decrease the surviving rate of crayfish after challenged by *E. ictaluri*. Crayfish injected with dsRNA against GFP, mock treated crayfish, and crayfish only challenged by *S. aureus* or *E. ictaluri* served as control.

In conclusion, a new *ddc* gene was identified from *P. clarkii,* and its expression patterns in crayfish hemocytes, hepatopancreas, gills, and intestine were clearly upregulated after being challenged with *S. aureus* or *E. ictaluri*. r*Pc*-DDC could efficiently catalyze L-dopa to produce dopamine *in vitro*. Additionally, r*Pc*-DDC could strongly bind to *S. aureus* and *E. ictaluri*. In addition, after *Pc-ddc* was knocked down, the number of surviving crayfish was clearly decreased after being challenged with *S. aureus* or *E. ictaluri*. These results indicate that *Pc*-DDC is an important immunomodulating enzyme in the neuroendocrine-immune system of crayfish.

## Acknowledgments

This work was supported by the National Natural Science

Foundation of China (Grant No. 31460698 and 31660260).

## References

[1] M. Sideri, S. Tsakas, E. Markoutsa, M. Lampropoulou, V.J. Marmaras, Innate immunity in insects: surface-associated dopa decarboxylase-dependent pathways regulate phagocytosis, nodulation and melanization in medfly haemocytes, Immunology 4 (2008) 528–537.

[2] P. Amparyup, W. Charoensapsri, A. Tassanakajon, Prophenoloxidase system and its role in shrimp immune responses against major pathogens, Fish Shellfish Immunol. 4 (2013) 990–1001.

[3] S. Kurata, Peptidoglycan recognition proteins in *Drosophila* immunity, Dev. Comp. Immunol. 1 (2014) 36–41.

[4] I. Eleftherianos, C. Revenis, Role and importance of phenoloxidase in insect hemostasis, J Innate Immun 1 (2011) 28–33.

[5] L. Cerenius, K. Söderhäll, The prophenoloxidase-activating system in invertebrates, Immunol. Rev. 198 (2004) 116–126.

[6] Z. Zhou, J. Yang, L. Wang, H. Zhang, Y. Gao, X. Shi, et al., A dopa decarboxylase modulating the immune response of scallop *Chlamys farreri*, PLoS One 4 (2011) e18596.

[7] Z. Zhou, L. Wang, X. Shi, F. Yue, M. Wang, H. Zhang, et al., The expression of dopa decarboxylase and dopamine beta hydroxylase and their responding to bacterial challenge during the ontogenesis of scallop *Chlamys farreri*, Fish Shellfish Immunol. 1 (2012) 67–74.

[8] S.E. Martelle, L.M. Raffield, N.D. Palmer, A.J. Cox, B.I. Freedman, C.E. Hugenschmidt, et al., Dopamine pathway gene variants may modulate cognitive performance in the DHS-Mind Study, Brain Behav. 4 (2016) e00446.

[9] R. Tehranian, S.E. Montoya, A.D. Van Laar, T.G. Hastings, R.G. Perez, Alpha-synuclein inhibits aromatic amino acid decarboxylase activity in dopaminergic cells, J. Neurochem. 4 (2006) 1188–1196.

[10] H. Verlinden, Dopamine signalling in locusts and other insects, Insect Biochem. Mol. Biol. 97 (2018) 40–52.

[11] D.F. Shih, C.D. Hsiao, M.Y. Min, W.S. Lai, C.W. Yang, W.T. Lee, et al., Aromatic L-amino acid decarboxylase (AADC) is crucial for brain development and motor functions, PLoS One 8 (2013) e71741.

[12] N.H. Neff, T.A. Wemlinger, A.M. Duchemin, M. Hadjiconstantinou, Clozapine modulates aromatic L-amino acid decarboxylase activity in mouse striatum, J. Pharmacol. Exp. Ther. 2 (2006) 480–487.

[13] Z. Liu, M. Li, Q. Yi, L. Wang, L. Song, The neuroendocrine-immune regulation in response to environmental stress in marine bivalves, Front. Physiol. 9 (2018) 1456.

[14] R.B. Hodgetts, S.L. O'Keefe, Dopa decarboxylase: a model gene-enzyme system for studying development, behavior, and systematics, Annu. Rev. Entomol. 51 (2006) 259–284.

[15] M.X. Wang, Z.Z. Cai, Y. Lu, H.H. Xin, R.T. Chen, S. Liang, et al., Expression and functions of dopa decarboxylase in the silkworm, *Bombyx mori* was regulated by molting hormone, Mol. Biol. Rep. 6 (2013) 4115–4122.

[16] Y. Arakane, J. Lomakin, R.W. Beeman, S. Muthukrishnan, S.H. Gehrke, M.R. Kanost, et al., Molecular and functional analyses of amino acid decarboxylases involved in cuticle tanning in *Tribolium castaneum*, J. Biol. Chem. 24 (2009) 16584–16594.

[17] M.M. Davis, D.A. Primrose, R.B. Hodgetts, A member of the p38 mitogen-activated protein kinase family is responsible for transcriptional induction of Dopa decarboxylase in the epidermis of *Drosophila melanogaster* during the innate immune response, Mol. Cell. Biol. 15 (2008) 4883–4895.

[18] S.M. Paskewitz, O. Andreev, Silencing the genes for dopa decarboxylase or dopachrome conversion enzyme reduces melanization of foreign targets in *Anopheles gambiae*, Comp. Biochem. Physiol. B Biochem. Mol. Biol. 4 (2008) 403–408.

[19] Z.Q. Du, BAX, a novel cell pro-apoptotic protein, involved in hemocytes early antiviral immune response in fresh water crayfish, *Procambarus clarkii*, Fish Shellfish Immunol. 55 (2016) 384–392.

[20] K. Wang, X.L. Shen, J.S. Jia, X.D. Yu, J. Du, S.H. Lin, et al., High-throughput sequencing analysis of microRNAs in gills of red swamp crayfish, *Procambarus clarkii* infected with white spot syndrome virus, Fish Shellfish Immunol. 83 (2018) 18–25.

[21] Z.Q. Du, J.J. Yuan, D.M. Ren, A novel single WAP domain-containing protein isoform with antibacterial relevance in *Litopenaeus vannamei*, Fish Shellfish Immunol. 2 (2015) 478–484.

[22] Z.Q. Du, X.C. Li, Z.H. Wang, X.F. Zhao, J.X. Wang, A single WAP domain (SWD)-containing protein with antipathogenic relevance in red swamp crayfish, *Procambarus clarkii*, Fish Shellfish Immunol. 1 (2010) 134–142.

[23] Z.Q. Du, J.F. Lan, Y.D. Weng, X.F. Zhao, J.X. Wang, BAX inhibitor-1 silencing suppresses white spot syndrome virus replication in red swamp crayfish, *Procambarus clarkii*, Fish Shellfish Immunol. 1 (2013) 46–53.

[24] Z.Q. Du, Y.H. Jin, Comparative transcriptome and potential antiviral signaling pathways analysis of the gills in the red swamp crayfish, *Procambarus clarkii* infected with White Spot Syndrome Virus (WSSV), Genet. Mol. Biol. 1 (2017) 168–180.

[25] X.C. Li, Z.Q. Du, J.F. Lan, X.W. Zhang, Y. Mu, X.F. Zhao, et al., A novel pathogen-binding gC1qR homolog, FcgC1qR, in the Chinese white shrimp, *Fenneropenaeus chinensis*, Dev. Comp. Immunol. 2 (2012) 400–407.

[26] Q. Ren, Z.Q. Du, M. Li, C.Y. Zhang, K.P. Chen, Cloning and expression analysis of an anti-lipopolysaccharide factor from giant freshwater prawn, *Macrobrachium rosenbergii*, Mol. Biol. Rep. 7 (2012) 7673–7680.

[27] Z.Q. Du, Q. Ren, X.F. Zhao, J.X. Wang, A double WAP domain (DWD)-containing protein with proteinase inhibitory activity in Chinese white shrimp, *Fenneropenaeus chinensis*, Comp. Biochem. Physiol. B Biochem. Mol. Biol. 2 (2009) 203–210.

[28] Z.Q. Du, Y.H. Jin, Molecular characterization and antibacterial activity analysis of two novel Penaeidin isoforms from pacific white shrimp, *Litopenaeus vannamei*, Appl. Biochem. Biotechnol. 8 (2015) 1607–1620.

[29] D. Tsukioka, S. Izumi, T. Adachi, Cloning and expression analysis of a novel tissue-specific dopa decarboxylase mRNA splicing variant in *Bombyx mori*, Biosci. Biotechnol. Biochem. 3 (2017) 555–557.

[30] T.R. Wright, Phenotypic analysis of the Dopa decarboxylase gene cluster mutants in *Drosophila melanogaster*, J. Hered. 3 (1996) 175–190.

[31] K. Kitahama, K. Ikemoto, A. Jouvet, S. Araneda, I. Nagatsu, B. Raynaud, et al., Aromatic L-amino acid decarboxylase-immunoreactive structures in human midbrain, pons, and medulla, J. Chem. Neuroanat. 2 (2009) 130–140.

[32] M. Moreira-Rodrigues, B. Sampaio-Maia, M. Pestana, Renal dopaminergic system activity in rat remnant kidney up to twenty-six weeks after surgery, Life Sci. 13–14 (2009) 409–414.

[33] J. Blechingberg, I.E. Holm, M.G. Johansen, A.D. Børglum, A.L. Nielsen, Aromatic l-amino acid decarboxylase expression profiling and isoform detection in the developing porcine brain, Brain Res. 1308 (2010) 1–13.

[34] J.L. Eberling, J.A. Roberts, S.E. Taylor, H.F. VanBrocklin, J.P. O'Neil, T.E. Nordahl, No effect of age and estrogen on aromatic L- amino acid decarboxylase activity in rhesus monkey brain, Neurobiol. Aging 3 (2002) 479–483.

[35] T. Takezako, K. Noda, E. Tsuji, M. Koga, M. Sasaguri, K. Arakawa, Adenosine activates aromatic L-amino acid decarboxylase activity in the kidney and increases dopamine, J. Am. Soc. Nephrol. 1 (2001) 29–36.

[36] H. Hayashi, H. Mizuguchi, H. Kagamiyama, Rat liver aromatic L-amino acid decarboxylase: spectroscopic and kinetic analysis of the coenzyme and reaction intermediates, Biochemistry 3 (1993) 812–818.

[37] J.A. Gilbert, L.M. Frederick, M.M. Ames, The aromatic-L-amino acid decarboxylase inhibitor carbidopa is selectively cytotoxic to human pulmonary carcinoid and small cell lung carcinoma cells, Clin. Cancer Res. 11 (2000) 4365–4372.

[38] I. Kokkinou, E. Nikolouzou, A. Hatzimanolis, E.G. Fragoulis, D. Vassilacopoulou, Expression of enzymatically active L-DOPA decarboxylase in human peripheral leukocytes, Blood Cells Mol. Dis. 1 (2009) 92–98.

[39] M.A. Flierl, D. Rittirsch, M. Huber-Lang, J.V. Sarma, P.A. Ward, Catecholamines-crafty weapons in the inflammatory arsenal of immune/inflammatory cells or opening pandora's box? Mol. Med. 3–4 (2008) 195–204.

[40] C.C. Chang, Z.R. Wu, C.M. Kuo, W. Cheng, Dopamine depresses immunity in the tiger shrimp *Penaeus monodon*, Fish Shellfish Immunol. 1 (2007) 24–33.

[41] J.T. Li, P.P. Lee, O.C. Chen, W. Cheng, C.M. Kuo, Dopamine depresses the immune ability and increases susceptibility to *Lactococcus garvieae* in the freshwater giant prawn, *Macrobrachium rosenbergii*, Fish Shellfish Immunol. 3 (2005) 269–280.